Available online at www.sciencedirect.com
SCIENCE DIRECT®
Journal of Sound and Vibration 276 (2004) 105–119
JOURNAL OF SOUND AND VIBRATION
www.elsevier.com/locate/jsvi

A complex filter for vibration signal demodulation in bearing defect diagnosis

Yuh-Tay Sheen*

Department of Mechanical Engineering, Southern Taiwan University of Technology, 1 Nan-Tai Street, Yung Kang City 710, Tainan County, Taiwan

Received 27 March 2003; accepted 2 August 2003

Abstract

In this paper, a complex filter for Hilbert transform is proposed to apply in the real-time vibration signal demodulation. The filter could provide a complex signal directly, as a function of both frequency and time, and the envelope could be derived from the absolute value of the complex signal. Three parameters, the scaling factor, center frequency and passband width, are designated to achieve the satisfactory properties of fast waveform convergence, constant passband gain and little phase distortion. Thus, a finite waveform interval of the proposed filter could be possibly applied in the vibration signal demodulation. From theoretical analysis and experimental studies, it is shown that the proposed filter could be effectively applied in the real-time vibration signal demodulation for a roller bearing system.

1. Introduction

In bearing defect diagnosis, the high-frequency resonance technique is always applied to the vibration signal demodulation [1–4]. In the range of a high-frequency system resonance, this technique takes advantage of the absence of low-frequency mechanical noise to demodulate a vibration signal and, therefore, provides a low-frequency demodulated signal with a high signal-to-noise ratio. In order to implement the high-frequency resonance technique, the Hilbert transform is often applied in vibration signal demodulation to provide a complex signal. Accordingly, the demodulated signal could be obtained from the absolute value of the complex signal.

*Tel.: +886-625-331-31, ext. 3522; fax: +886-624-250-92.
E-mail address: syt@mail.stut.edu.tw (Y.-T. Sheen).

0022-460X/$ - see front matter
doi:10.1016/j.jsv.2003.08.007

A recent method for detecting vibration envelope is based on the Morelet wavelet that constructs a Hilbert transform pair that calls for two wavelet transforms, where one wavelet is the Hilbert transform of the other. However, the Morelet wavelet could only be an orthogonal narrow filter [5]. Huang [6] proposes an algorithm for the linear combination of Morlet wavelets to apply in detecting vibration signal envelope. However, it is inconvenient to apply in practice for the transformation function expressed in the combination function form. In addition, the normalized coefficient for the linear combination of analysis wavelets also needs to be determined, as the case may be. Nikolaou and Antoniadis [7] base on the use of a complex shifted Morlet wavelet family to construct a matrix from the absolute value of wavelet transform for a vibration signal. By sorting the maximum values of each column in the matrix, an envelope of the vibration signal could be derived and be capable of detecting the appearance of each impulse in the frequency band. But there are very serious distortions in the amplitude and phase.

The modern signal analysis for defect detection is applied to determine the instantaneous frequency of vibration signal [8–11]. The wavelet transform is most often used because of a feature of time-frequency localization that is capable of exhibiting the instantaneous frequencies of vibration signal and gives a description of how energy distribution over the changes of frequencies from one instance to another. To detect localized defects of bearing, the magnitude variation of wavelet transform at different dilations varies periodically at a rate of the characteristic frequency of a certain defect. However, it is inconvenient to figure out the characteristic frequency and location of a defect, especially for the case of multiple-type defects.

In this paper, a complex filter for Hilbert transform is proposed to apply in the real-time vibration signal demodulation and capable of presenting the instantaneous frequency of its envelope. There are three parameters for designating the proposed filter. By tuning up these parameters, the passband properties, such as the filtering bandwidth, slope attenuation and cut-off frequencies, could be adjusted and designated. Because the envelope is expressed as a function of both frequency and time, the envelope function could present the instantaneous frequency to depict how energy distribution over the changes of passband from one instance to another. In addition, the envelope spectrum could describe how energy distribution over the changes of passband from one instantaneous frequency to another.

2. A complex filter for Hilbert transform

2.1. Basic concept

In the diagnosis of a bearing system, there is the amplitude modulation occurred in measured signals, and thus the frequency-translation property would be presented in the vibration spectra. The phenomenon of amplitude modulation is because a high-frequency carrier signal is varied by a low-frequency modulating signal. Thus, the modulated signal could be the product of the modulating signal with the carrier signal. The modulating signal is the impacts caused by defects of a bearing and could be represented by bursts of exponentially decaying vibration. Thus, its spectrum would be expanded in a frequency band. The carrier signal is a combination of the resonance frequencies of the bearing or even of the mechanical system. The frequency of modulating signal would be always much smaller than that of carrier signal. Accordingly, the

modulated signal would also be expanded in frequency band whose center frequency would be at the frequencies of carrier signal. To deal with this phenomenon of amplitude modulation, the high-frequency resonance technique is introduced, which is tried to derive the low-frequency modulating signal from the modulated signal by means of filtering out the high-frequency carrier signal.

In the high-frequency resonance technique, a complex filter for Hilbert transform with the properties of both a constant passband gain and perfect orthogonality is required for bandpass-filtering around resonance frequency. If a complex signal is derived from the convolution of a vibration signal and the complex filter, an envelope signal could be the absolute value of the complex signal. Thus, the complex filter could be taken to be the form

$$h(t) = h_r(t) + \mathrm{j}h_i(t), \tag{1}$$

where $h_i(t)$ is the Hilbert transform for $h_r(t)$. In order to realize such a complex filter for Hilbert transform, some properties are discussed as follows:

(1) If $h_r(t)$ is an even function, $h_i(t)$ would be odd.
(2) Function $h_i(t)$ should be orthogonal to $h_r(t)$.
(3) Both $h_r(t)$ and $h_i(t)$ should be bandpass filters.

In the following, such a complex filter for Hilbert transform is first proposed and some properties of the complex filter are then discussed.

2.2. Theoretical study

In this paper, a complex filter for Hilbert transform is proposed and defined as

$$h_{a,f_C,f_W}(t) = \frac{1}{\mathrm{j}\pi t}\,\mathrm{e}^{-(t/a)^2}(\mathrm{e}^{-\mathrm{j}2\pi(f_C - f_W/2)t} - \mathrm{e}^{-\mathrm{j}2\pi(f_C + f_W/2)t}), \tag{2}$$

where a, f_C and f_W are the scaling factor, the center frequency and the passband width, respectively. It is noted that the complex filter $h_{a,f_C,f_W}(t)$ in Eq. (2) comprises three parameters for adjustment and designation of the filtering passband.

The Fourier transform of this filter function could then be expressed as

$$H(f) = erf\left(a\left(f - f_C - \frac{f_W}{2}\right)\pi\right) - erf\left(a\left(f - f_C + \frac{f_W}{2}\right)\pi\right), \tag{3}$$

where $erf(z) = 2/\sqrt{\pi}\int_0^z \mathrm{e}^{-f^2}\,\mathrm{d}f$ is the error function. It is found that $H(f)$ has a passband with a constant gain and two cut-off frequencies at $f_C - f_W/2$ and $f_C + f_W/2$. In addition, an increase in scaling factor a is associated with a sharper cut-off. Thus, with a proper selection of scaling factor a, the filter function could be an excellent bandpass filter.

On the other hand, the real part and the imaginary part of the complex filter $h_{a,f_C,f_W}(t)$ are $h_r(t)$ and $h_i(t)$, respectively, and could be written as

$$h_r(t) = \frac{1}{\pi t}\,\mathrm{e}^{-(t/a)^2}\left[\sin\left(2\pi\left(f_C + \frac{f_W}{2}\right)t\right) - \sin\left(2\pi\left(f_C - \frac{f_W}{2}\right)t\right)\right], \tag{4a}$$

and

$$h_i(t) = \frac{1}{\pi t} e^{-(t/a)^2} \left[\cos\left(2\pi \left(f_C + \frac{f_W}{2} \right) t \right) - \cos\left(2\pi \left(f_C - \frac{f_W}{2} \right) t \right) \right]. \tag{4b}$$

It is easy to verify that the imaginary part $h_i(t)$ is orthogonal to its own real part $h_r(t)$. Therefore, the imaginary part $h_i(t)$ would be the Hilbert transform for its own real part $h_r(t)$.

From the above, it is found that the complex filter in Eq. (2) possesses the properties of bandpass filtering and orthogonality. So that function $h_{a,f_C,f_W}(t)$ could be used to form a Hilbert transform pair that is capable of applying in the high-frequency resonance technique.

The filtering operation of Hilbert transform for a vibration signal $x(t)$ could then be described by the convolution integral of $x(t)$ and $h_{a,f_C,f_W}(t)$

$$y_{a,f_C,f_W}(t) = \int_{-\infty}^{\infty} x(\tau) h_{a,f_C,f_W}(t-\tau)\, d\tau. \tag{5}$$

The above operation is linear and the filtered signal $y_{a,f_C,f_W}(t)$ is complex. In addition, the imaginary part of $y_{a,f_C,f_W}(t)$ also is the Hilbert transform of its own real part. Therefore, an envelope could be derived from the absolute value of $y_{a,f_C,f_W}(t)$ and an envelope transformation is defined as

$$e_{a,f_C,f_W}(t) = \left| \int_{-\infty}^{\infty} x(\tau) h_{a,f_C,f_W}(t-\tau)\, d\tau \right|. \tag{6}$$

From the above envelope transformation, an envelope of the vibration signal $x(t)$ could be derived. When properly selecting the scaling factor a and the passband width f_W, the envelope function $e_{a,f_C,f_W}(t)$ could be used to depict how energy distribution over the changes of passband from one instance to another. In addition, location and width of the filtering passband could be determined by the center frequency f_C and the passband width f_W, respectively. Thus, the envelope function $e_{a,f_C,f_W}(t)$ possesses the feature of time-frequency localization. The instantaneous frequencies, which correspond to the selection of center frequency of the filtering passband, of the envelope could be derived and capable of sweeping the filtering passband from a low-frequency band to a high-frequency band.

Furthermore, the frequency information of $e_{a,f_C,f_W}(t)$ can be derived from its Fourier transform

$$E_{a,f_C,f_W}(f) = \Im\{e_{a,f_C,f_W}(t)\}, \tag{7}$$

where $\Im$ denotes the Fourier transform. It should be noted that the above equation could be used to describe how energy distribution over the changes of filtering passband from one instantaneous frequency to another. In comparison with the envelope function $e_{a,f_C,f_W}(t)$, the envelope spectrum $E_{a,f_C,f_W}(f)$ would be capable of giving a clearer view of characteristic frequencies for vibration signals. Such a view would be helpful to point out the location of defects in system diagnosis.

2.3. Parameter characteristics

For the purpose of practically applying the complex filter $h_{a,f_C,f_W}(t)$, as shown in Eq. (2), in the high-frequency resonance technique, the characteristics of function parameters would be investigated in the following.

From Eq. (3), the passband designation of complex filter $h_{a,f_C,f_W}(t)$ could be a function of a, f_C and f_W. For selected values of f_C and f_W, a decrease of scaling factor a of $h_{a,f_C,f_W}(t)$ would increase waveform convergent speed but decrease slope attenuation. As shown in Fig. 1, the waveform convergent speed in the case of scaling factor $a = 0.002$ is faster than that in the case of scaling factor $a = 0.02$. However, as shown in Fig. 2, the slope attenuation in the case of $a = 0.02$ is sharper than that in the case of scaling factor $a = 0.002$. Therefore, it is shown that an increase of slope attenuation can be traded off for an increase of waveform convergent speed, and vice versa. An increase in scaling factor a is associated with both sharp cut-off and slow convergent speed. Finally, it should be noted that both passband quality and waveform convergent speed of the complex filter $h_{a,f_C,f_W}(t)$ are no relation with f_C and f_W, but vary little under the constraint of scaling factor $a \geqslant 0.007$.

On the other hand, the selection of passband width f_W is, in general, dependent on the bandwidth of impulse response of defects, and the selection of center frequency f_C decides the location of filtering passband. An increase of f_C would be capable of sweeping a filtering passband from a low-frequency band to a high-frequency band. For most cases in a mechanical system, the passband width could be $f_W = 3$ kHz and the center frequency could be in the range of $3\text{ kHz} \leqslant f_C \leqslant 11$ kHz. It is noted that the center frequency should be smaller than the Nyquist frequency. Accordingly, when applying in the high-frequency resonance technique, the envelope transformation as shown in Eq. (6), would not trouble to decide the filtering passband and could be convenient for the end user.

In practice, the waveform interval of $h_{a,f_C,f_W}(t)$ taken to apply in signal processing must be limited. However, both a sharp cut-off and a better waveform convergence are necessary for a better passband quality. Besides, the waveform interval would be increased with scaling factor a to achieve both a sharp cut-off and a better waveform convergence. Accordingly, the waveform interval should be as long as possible for a better passband quality. But the computing burden would be increased with the waveform interval. Nevertheless, under proper selections of both scaling factor a and waveform interval of $h_{a,f_C,f_W}(t)$, the passband quality could be still guaranteed.

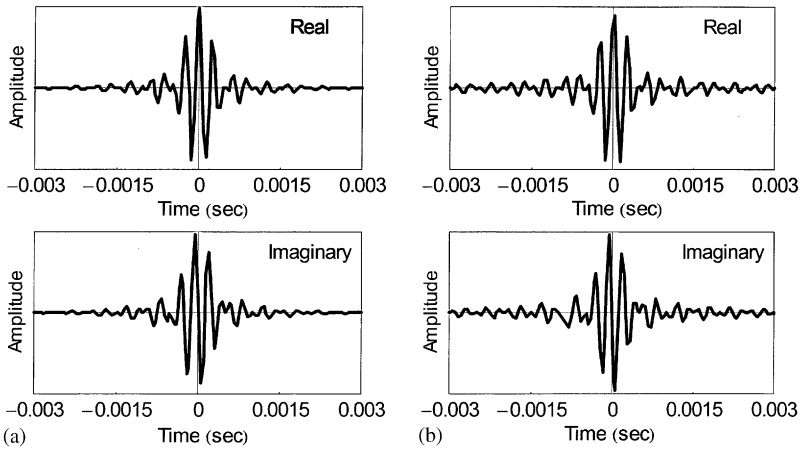

Fig. 1. The waveform of $h_{a,f_C,f_W}(t)$. (a) $a = 0.002$ and (b) $a = 0.02$.

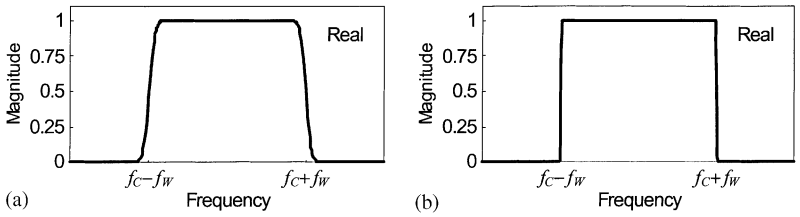

Fig. 2. The spectrum of $h_{a,f_C,f_W}(t)$. (a) $a = 0.002$ and (b) $a = 0.02$.

It is suggested that the waveform interval of $h_{a,f_C,f_W}(t)$ is chosen to be more than 0.01 s and then the scaling factor a could be constrained in the range $0.007 \leqslant a \leqslant 0.015$.

3. Computer algorithm

For the purpose of implementation in computer, an algorithm for the above theoretical study is divided into the following steps.

(1) Based on the system characteristics, specify the parameters of sampling rate T, scaling factor a, passband width f_W and a range of center frequency f_C. The complex filter $h_{a,f_C,f_W}(t)$ with a finite waveform interval $2KT$ could be expressed in the discrete form as

$$h_{a,f_C,f_W}(k) = \frac{1}{\mathrm{j}\pi kT} \mathrm{e}^{-(kT/a)^2} (\mathrm{e}^{-\mathrm{j}2\pi(f_C - f_W/2)kT} - \mathrm{e}^{-\mathrm{j}2\pi(f_C+f_W/2)kT}), \tag{8}$$

where $k(-K \leqslant k \leqslant K)$ is a number to be located in the waveform.

(2) For a given signal sequence $x(m)$, $0 \leqslant m \leqslant M$, the filtering operation of Hilbert transform could be derived from the convolution of $x(k)$ and $h_{a,f_C,f_W}(k)$,

$$y_{a,f_C,f_W}(n) = \sum_{m=0}^{M} x(n-m) h_{a,f_C,f_W}(m) T, \tag{9}$$

where $y_{a,f_C,f_W}(n)$ is complex and $0 \leqslant n \leqslant M + 2K$.

(3) The envelope of signal sequence $x(m)$ can be derived from the absolute value of $y_{a,f_C,f_W}(n)$,

$$e_{a,f_C,f_W}(n) = |y_{a,f_C,f_W}(n)|. \tag{10}$$

(4) For a finite envelope sequence $e_{a,f_C,f_W}(n)$, the operation of multiplying an envelope $e_{a,f_C,f_W}(t)$ by the Hanning windows $w(t)$ is used in the estimation of envelope spectrum $E_{a,f_C,f_W}(f)$. The Hanning window of length $M + 2K$ is given by [12]

$$w(n) = \frac{1}{2}\left(1 - \cos\frac{2\pi n}{M+2K}\right). \tag{11}$$

(5) Taking FFT for the windowed envelope sequence, the finite-interval envelope spectrum $\hat{E}_{a,f_C,f_W}(f)$ could be obtained. It follows that $\hat{E}_{a,f_C,f_W}(f)$ is the convolution of the Fourier

transform of $e_{a,f_C,f_W}(t)$ and $w(t)$ [12],

$$\hat{E}_{a,f_C,f_W}(f) = \sum_{-\infty}^{\infty} E_{a,f_C,f_W}(f-g)W(g)\,\mathrm{d}g, \tag{12}$$

where the spectral window $W(f)$ is the Fourier transform of the Hanning window $w(t)$. Thus, $\hat{E}_{a,f_C,f_W}(f)$ is an estimation of envelope spectrum $E_{a,f_C,f_W}(f)$.

4. Evaluation and results

In this section, the above algorithm for computer implementation is tested on a simulated pulse train. Each pulse is modulated by two signal harmonic frequencies with an exponential decay. This signal could be used to model an impulse response signal modulated with two simplified system resonance frequencies and is expressed as

$$x(k) = \mathrm{e}^{-\alpha k t'}(\sin 2\pi f_1 kT + \sin 2\pi f_2 kT), \tag{13}$$

with

$$t' = \mathrm{mod}\left(kT, \frac{1}{f_0}\right), \tag{14}$$

where $\alpha = 800$, $f_0 = 100$ Hz, $f_1 = 3$ kHz and $f_2 = 8$ kHz are the exponential frequency, the modulating frequency and two carrier frequencies, respectively. Let the sampling interval be $T = 1/25,000$ s and Fig. 3 shows the waveform and spectrum of simulated signal. In the spectrum, peaks at 3 and 8 kHz are corresponding to two resonance frequencies. Fig. 4 is the signal after adding a significant level of Gaussian noise. Its signal-to-noise ratio, i.e., the variance ratio of signal to noise, is 0.257. The impulse train is almost buried in the noise.

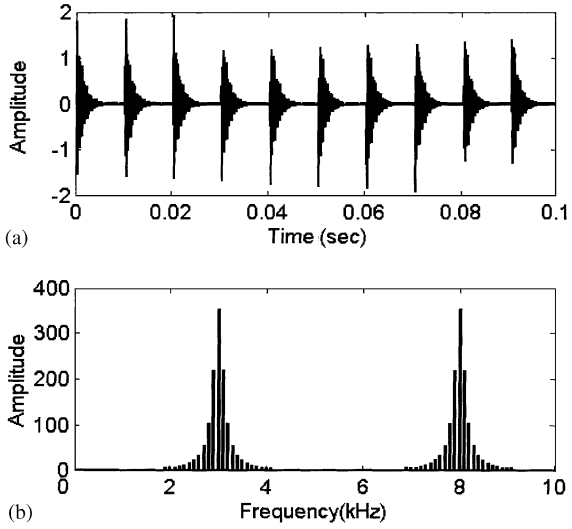

Fig. 3. (a) The waveform of simulated signal $x(k)$ and (b) the spectrum of $x(k)$.

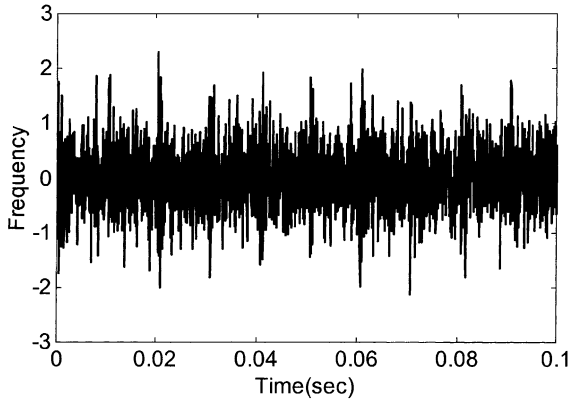

Fig. 4. The simulated signal $x(k)$ with additive Gaussian noise.

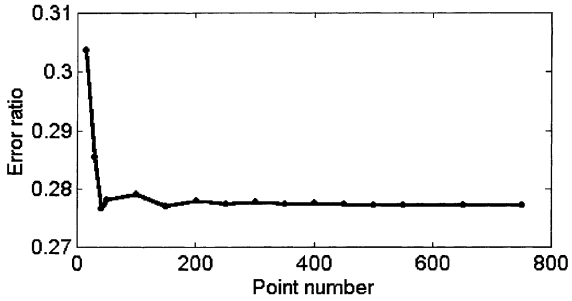

Fig. 5. The error ratio for measuring error between the modulating signal and the envelope.

In order to analyze the effect of envelope transformation with the complex filter composed of a finite waveform interval, an error ratio for measuring the error between the modulating signal and the envelope is defined as

$$error\ ratio = \frac{\text{standard deviation of error}}{\text{standard deviation of modulating signal}}. \tag{15}$$

When applying the complex filter $h_{a,f_C,f_W}(k)$ in Eq. (8) to demodulate the modulated signal $x(t)$, the envelope $e_{a,f_C,f_W}(n)$ could be obtained according to Eq. (10). Based on the spectrum in Fig. 3(b), the parameter values are taken to be scaling factor $a = 0.007$, center frequency $f_C = 3$ kHz and passband width $f_W = 3$ kHz. The selected passband would cover from the low cut-off frequency at 1.5 kHz to the high cut-off frequency at 4.5 kHz. Under different waveform interval, the envelope for the modulated signal $x(k)$ in Eq. (13) is derived and the error ratio is shown in Fig. 5. It is found that the error ratios are almost saturated when a waveform interval of complex filter is greater than 0.01 s (about 250 points). With a waveform interval being 0.01 s, Fig. 6 shows waveforms of both modulating signal and the demodulated signal and they are very close. The same result for their spectra in both amplitude and phase is shown in Fig. 7. Under the condition of the same parameter selection, the result of envelope transformation of the signal in Fig. 4 is

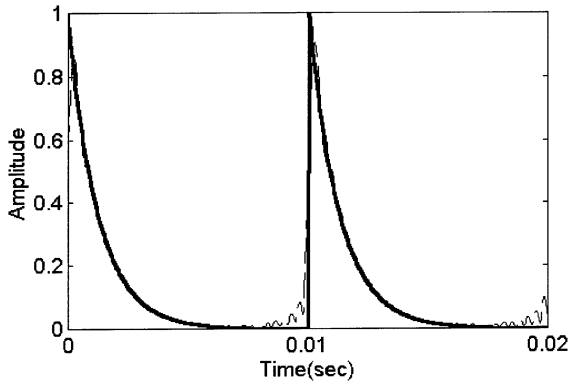

Fig. 6. The waveform (the modulating signal: ——, the envelope: _ _ _).

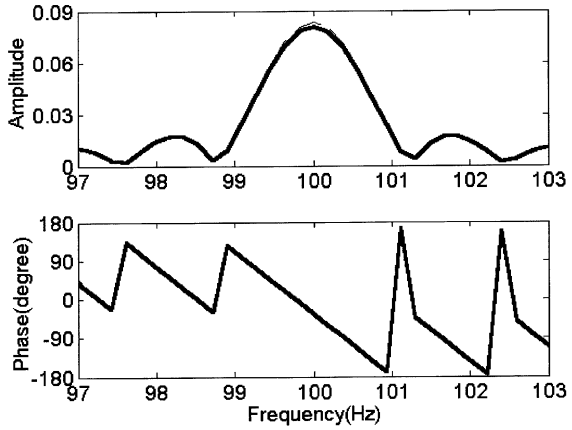

Fig. 7. The spectra of the waveform in Fig. 6 (the modulating signal: ——, the envelope: _ _ _).

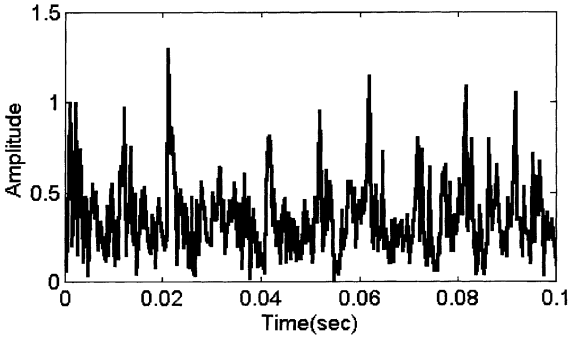

Fig. 8. The envelope of the signal in Fig. 4.

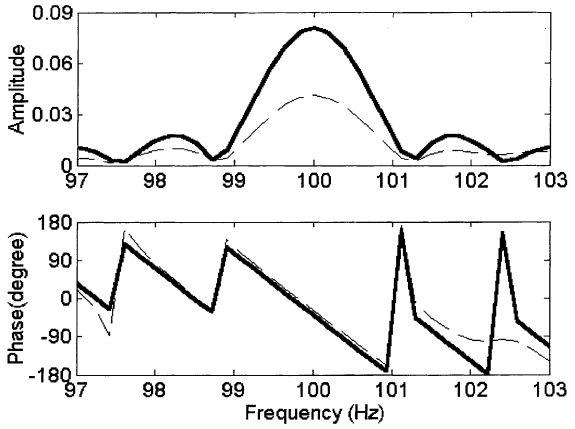

Fig. 9. The spectra (the modulating signal: ——, the envelope of the signal in Fig. 4: _ _ _).

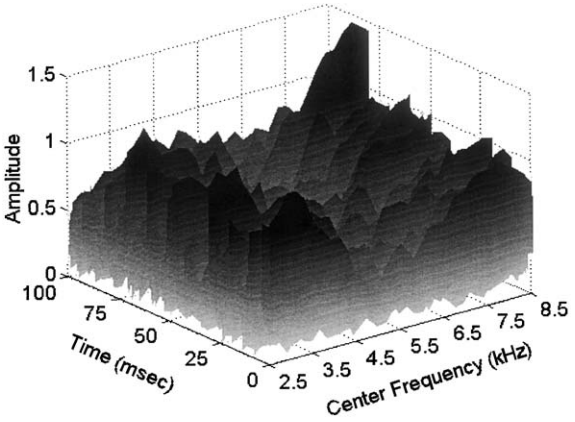

Fig. 10. 3D envelope illustration for the signal in Fig. 4.

shown in Fig. 8 and the impulses can be found in the figure. However, the period of the demodulated signal is not very clear because of the influence of the significant noise. Fig. 9 shows the spectrum of the waveform in Fig. 8. In comparison with Fig. 8, Fig. 9 shows a clear view of frequency information for the demodulated signal despite a significant level of Gaussian noise. Thus, the spectrum of the demodulated signal is more useful in finding the modulating signal. The influence of the noise on the demodulated signal is the spectral amplitude significantly decayed. It is noted that the phase around the frequency of modulating signal is also accurate in spite of a significant level of Gaussian noise added to the simulated signal. In addition, there are the same results for the envelope transformation in a passband containing the other resonance frequency at 8 kHz. Thus, the envelope transformation in Eq. (10) is excellent in vibration signal demodulation, especially in the phase response.

Furthermore, when sweeping the center frequency in the range $3\ \text{kHz} \leqslant f_C \leqslant 11\ \text{kHz}$ for the envelope transformation of the signal in Fig. 4, the 3D envelope illustration, as shown in Fig. 10, could describe the envelope changes over the passband sweeping from one instance to another. Fig. 11 shows the 3D envelope spectrum which gives a clear view of the modulating signal

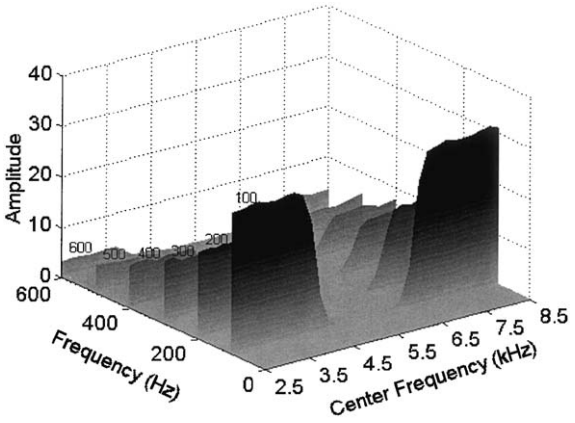

Fig. 11. 3D envelope spectrum of the 3D envelope in Fig. 10.

frequency and their harmonic frequencies. In comparison with Fig. 10, Fig. 11 would present more useful information of characteristic frequency for diagnosis in spite of a significant level of Gaussian noise added to the simulated signal. In addition, the amplitude in Fig. 11 is decayed rapidly in the range of passband between $f_C = 4.5$ and 6.5 kHz, because this range is corresponding with the passbands uncovering any resonance frequencies. It is noted that the cross-section along the center-frequency axis is similar to the spectrum in Fig. 3(b). Accordingly, the range of center frequency would determine the number of resonance frequencies contained.

5. Experimental study

In this section, the complex filter $h_{a,f_C,f_W}(k)$ in Eq. (8) is applied to demodulate vibration signals of tapered roller bearings (SKF type 32208) at running speed 800 r.p.m. There are initial defects, as described in Ref. [3], occurring on roller, outer race and inner race, respectively. The parameter values are taken to be $a = 0.007$, $f_W = 3$ kHz, and 3 kHz$\leqslant f_C \leqslant$11 kHz. All computations are carried out on an IBM compatible computer with a TMS320C32 DSP interface card. The envelope transformation is coded in C and implemented on TMS320C32 DSP interface card with a sampling rate 25 kHz. In order to process the vibration signals in real-time, the finite number of function waveform is taken to be 250 points (or 0.01 s). For the purpose of demonstration, 8192 points of envelope with a sampling rate 3.125 kHz are calculated to construct the 3D envelope spectrum between instantaneous frequency and center frequency of filtering passband. The envelope spectra of vibration signals can be derived from DSP card and is shown by using Builder C language for user-friendly programming under Microsoft Windows.

The characteristic frequencies of tested bearings for roller, outer- and inner-race are 77.3, 94.6 and 131.9 Hz, respectively. In Fig. 12, the 3D envelope illustration between time and center frequency for vibration signals of roller bearing with single roller defect is shown. Its 3D envelope spectrum is shown in Fig. 13. Along the frequency axis of co-ordinate, Fig. 13 clearly shows the characteristic frequency and its harmonic frequencies. On the other hand, the 3D diagrams, as shown in Figs. 14 and 15, are shown for a normal bearing to correspond to the vibration envelope

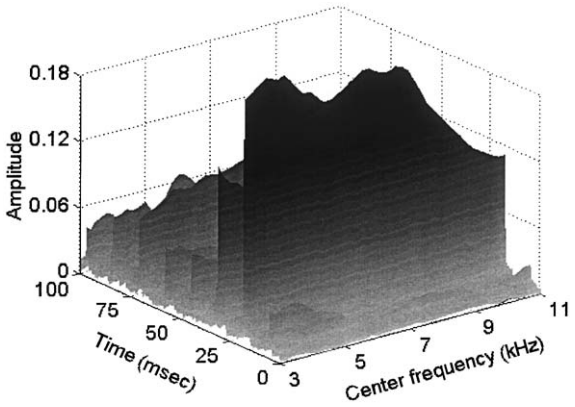

Fig. 12. 3D envelope illustration for roller bearing with a roller defect at running speed 800 r.p.m.

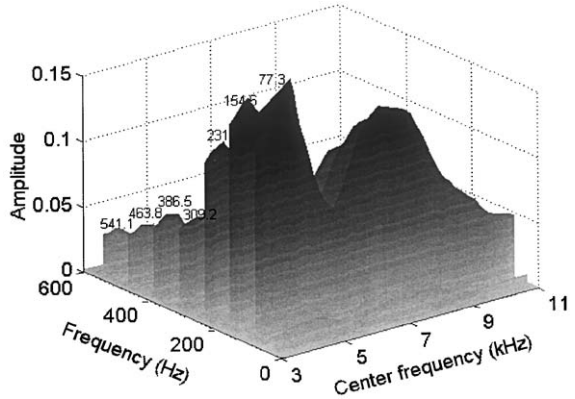

Fig. 13. 3D envelope spectrum of the 3D envelope in Fig. 12.

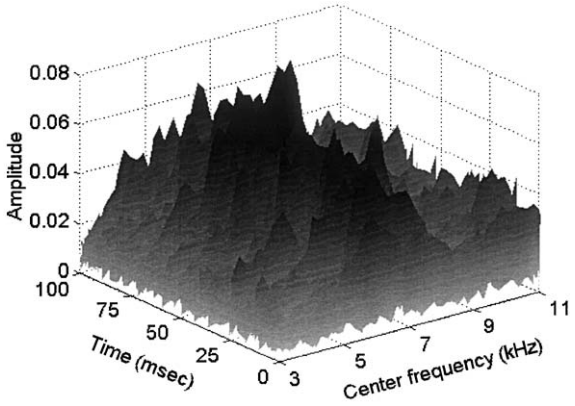

Fig. 14. 3D envelope illustration for normal bearing at running speed 800 r.p.m.

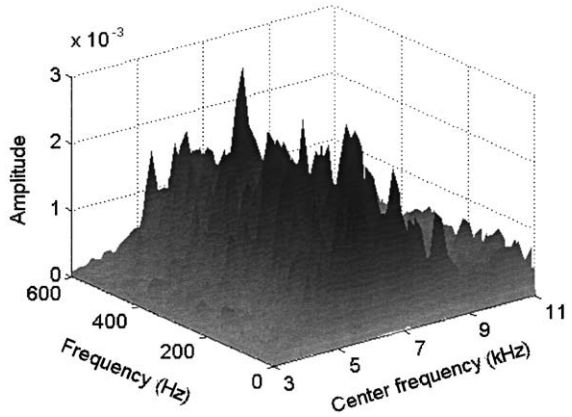

Fig. 15. 3D envelope spectrum of the 3D envelope in Fig. 14.

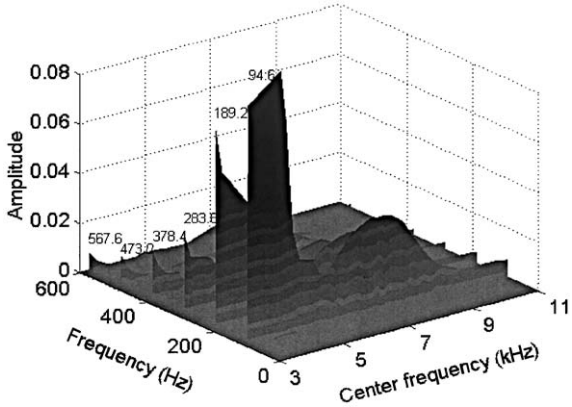

Fig. 16. 3D envelope spectrum for roller bearing with an outer-race defect at running speed 800 r.p.m.

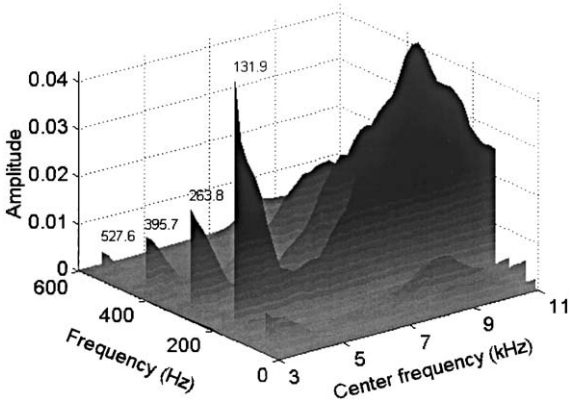

Fig. 17. 3D envelope spectrum for roller bearing with an inner-race defect at running speed 800 r.p.m.

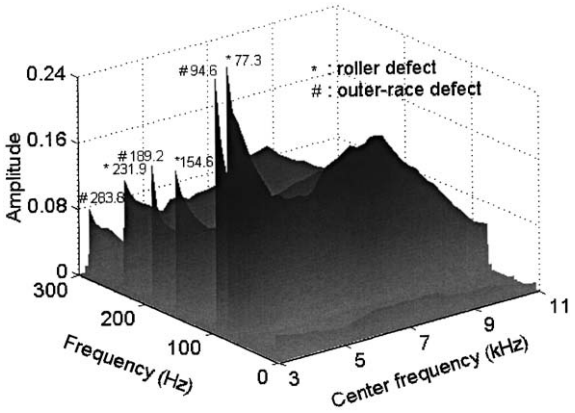

Fig. 18. 3D envelope spectrum for roller bearing with multiple-type defects at running speed 800 r.p.m.

and its spectrum. In comparison with Figs. 12 and 13 for a roller defect bearing, Figs. 14 and 15 for normal bearing show obviously a different kind of pattern in which there is no periodic slices appeared. Furthermore, the 3D envelope spectrum would present more useful information about the characteristic frequency for bearing defect diagnosis.

The 3D envelope spectra, as shown in Figs. 16 and 17, show for roller bearings with an outer-race defect and an inner-race defect, respectively. The characteristic frequencies and its harmonic frequencies for defects are clearly found. Similar result for a roller bearing with multiple-type defects, both roller and outer-race defects, is shown in Fig. 18. Accordingly, the 3D envelope spectrum would be also useful for bearing defect diagnosis in location of multiple-type defects.

6. Discussion

Theoretically, there are no ripples in filtering passband for the complex filter. However, a finite waveform interval of the complex filter should, in practice, be taken. In addition, the arithmetic round-off errors would be occurred in computation. These shortcomings would cause the filtering passband distorted and the Gibbs phenomenon occurring in the filtering passband. Accordingly, the orthogonality between the real part and the imaginary part would be distorted; thereby the characteristic of Hilbert transform is twisted. Nevertheless, these problems could be minimized under the condition of properly selecting both the scaling factor and the waveform interval for the complex filter. According to the suggestion in Section 2.3, it is found that the suggested values for the parameters of complex filter could obtain both a fast convergent waveform and a sharp cut-off. It would be helpful to solve the above shortcomings.

When using Eq. (10) for envelope transformation, there is an advantage of reducing the computing burden. It is because that the vibration frequency of the envelope, in comparison with that of modulated signal, would become much lower, and thereby the sampling rate for the envelope could also be reduced. Thus, most items in computing the envelope sequence could be neglected. Accordingly, the computing speed for finding the envelope sequence could be much increased. It would, in practice, be helpful to take a longer waveform interval of the complex filter

into account to achieve a better waveform convergence. Accordingly, the complex filter could be possibly applied in real-time signal processing, and the envelope transformation would be capable of using in practice to demodulate vibration signals of a mechanical system.

Besides, real part of the filtering operation, as shown in Eq. (4a), could be a bandpass filter for a vibration signal and possesses the same satisfactory properties as those of the envelope transformation. At the same time, the imaginary part could also be a bandpass filter and be the Hilbert transform of the real part. Thus, the complex filter could also be used in design of a bandpass filter, and provides an easy way in both passband selection and slope attenuation designation.

7. Conclusion

This paper proposes a complex filter for Hilbert transform to apply in vibration signal demodulation. There are three parameters for designating the complex filter to achieve satisfactory properties, which are the scaling factor, the center frequency of passband, and the passband width. Both the scaling factor and the waveform interval are suggested in the paper to designate the complex filter. Thus, the passband quality for the complex filter can be guaranteed with the suggested values. In addition, the complex filter provides an easy way to sweep filtering passband from a low-frequency band to a high-frequency band. It is convenient for the envelope transformation to apply in practice and there is an advantage of minimizing the interventions by the end user.

References

[1] P.D. McFadden, J.D. Smith, Vibration monitoring of rolling element bearings by the high-frequency resonance technique—a review, *Tribology International* 17 (1984) 1–18.
[2] Y.-T. Su, S.-J. Lin, On initial fault detection of a tapered rolling bearing: frequency domain analysis, *Journal of Sound and Vibration* 155 (1992) 75–84.
[3] Y.-T. Su, Y.-T. Sheen, On the detectability of roller bearing damage by frequency analysis, *Proceedings of the Institution of Mechanical Engineers, Part C: Journal of Mechanical Engineering Science* 207 (1993) 23–32.
[4] J. Shiroishi, Y. Li, S. Liang, T. Kurfess, S. Danyluk, Bearing condition diagnostics via vibration and acoustic emission measurement, *Mechanical Systems and Signal Processing* 11 (5) (1997) 693–705.
[5] C.C. Liu, G.Z. Qiu, A method based Morlet wavelet for extracting vibration signal envelope, in: *2000 Fifth International Conference on Signal Processing Proceedings*, 21–25 August, 2000, Beijing, China, pp. 337–340.
[6] D. Huang, A wavelet-based algorithm for the Hilbert transform, *Mechanical Systems and Signal Processing* 10 (2) (1996) 125–134.
[7] N.G. Nikolaou, I.A. Antoniadis, Demodulation of vibration signals generated by defects in rolling element bearings using complex shifted Morlet wavelets, *Mechanical Systems and Signal Processing* 16 (4) (2002) 677–694.
[8] C.J. Li, J. Ma, Wavelet decomposition of vibrations for detection of bearing-localized defects, *NDT&E International* 30 (3) (1997) 143–149.
[9] J. Lin, L. Qu, Feature extraction based on Morlet wavelet and its application for mechanical fault diagnosis, *Journal of Sound and Vibration* 234 (1) (2000) 135–148.
[10] B. Liu, S.-F. Ling, Machinery diagnosis based on wavelet packets, *Journal of Vibration and Control* 3 (2001) 5–17.
[11] W.J. Wang, Wavelets for detecting mechanical faults with high sensitivity, *Mechanical Systems and Signal Processing* 15 (4) (2001) 685–696.
[12] J.S. Bendat, A.G. Piersol, *Engineering Applications of Correlation and Spectral Analysis*, Wiley, New York, 1980.